Improving Ocean Angular Momentum Estimates Using a Model Constrained by Data

Rui M. Ponte[1], Detlef Stammer[2] and Carl Wunsch[3]

[1]Atmospheric and Environmental Research, Inc.
[2]Scripps Institution of Oceanography
[3]Massachusetts Institute of Technology

Abstract

Ocean angular momentum (OAM) calculations using forward model runs without any data constraints have recently revealed the effects of OAM variability on the Earth's rotation. Here we use an ocean model and its adjoint to estimate OAM values by constraining the model to available ocean data (altimetry, monthly hydrography, and sea surface temperature). The optimization procedure yields substantial changes in OAM, related to adjustments in both motion and mass fields, as well as in the wind stress torques acting on the ocean. Constrained and unconstrained OAM values are discussed in the context of closing the planet's angular momentum budget. The estimation procedure yields noticeable improvements in the agreement with the observed Earth rotation parameters, particularly at the seasonal time scale. This comparison with Earth rotation measurements provides a stringent independent consistency check on the estimated ocean state and underlines the importance of ocean state estimation for quantitative studies of the variable large-scale oceanic mass and circulation fields, including those on OAM.

Motivation

• Check impact on OAM values of ocean state estimation procedures

• Assess value of estimation procedure on improving OAM estimates, in the context of the planet's angular momentum budget

• Check the efficacy of the optimization scheme in producing better large-scale ocean circulation and mass fields

Ocean model and optimization scheme

• MIT ocean general circulation model on 2x2 degree horizontal grid and 23 vertical levels

• forced by surface atmospheric fluxes from NCEP/NCAR reanalysis (daily heat and freshwater fluxes; twice-daily wind stresses; no pressure forcing)

• daily averaged velocity and bottom pressure fields for 6-year period (1992-1997)

• adjoint method used to constrain model with TOPEX/ Poseidon and ERS-1/2 daily sea surface height anomalies, monthly mean hydrography, and sea surface temperature

(for full details on the MIT model and optimization scheme, and other analyses of the output used here, see nearby poster by Stammer et al.)

Calculation of OAM

OAM vector L:

$$\mathbf{L} = \mathbf{L^P} + \mathbf{L^V} = \int_V \rho\, \mathbf{r} \times (\Omega \times \mathbf{r} + \mathbf{v})\, dV$$

$\mathbf{L^P}$ — matter term due to solid body rotation, related to bottom pressure fields (p_b)

$\mathbf{L^V}$ — motion term due to velocities relative to solid Earth

ρ, V — ocean density and volume

$\mathbf{r}$ — position vector

Ω — Earth's mean rotation vector

$\mathbf{v}$ — relative velocity vector

Bottom pressure p_b:

$$p_b = g\,(\rho_0\,\zeta + \int_{-H}^{0} \rho\, dz)$$

where sea level ζ is corrected for volume effects due to changes in steric height

Three OAM components:

L_1, L_2 — components about equatorial axes, relevant for polar motion or wobble

L_3 — components about principal rotation axis, relevant for length of day (LOD) variations

Impact of optimization on OAM values

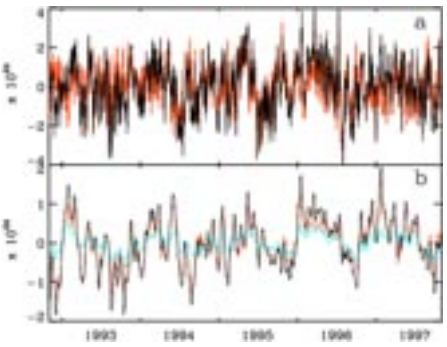

Figure 1. (a) Time series of L_2 (kg m^2 s^{-1}) starting in November 1, 1992. Unconstrained values are in red, constrained values in black. **(b)** Constrained minus unconstrained values for L_2 (black), L_2^P (red), and L_2^V (blue).

The impact of the estimation scheme is clearly seen, with peak-to-peak differences amounting to 50% of the signal. Difference curves are much smoother than the original OAM series, indicating the stronger impact of the data constraints on the longer time scales. The weak high-frequency changes are likely related to the relatively sparse observations used as constraints: global ocean coverage by T/P takes nearly 10 days. The amplitude of the annual cycle is enhanced by the optimization. Both L^V and L^P contribute, albeit changes in L^P are larger.

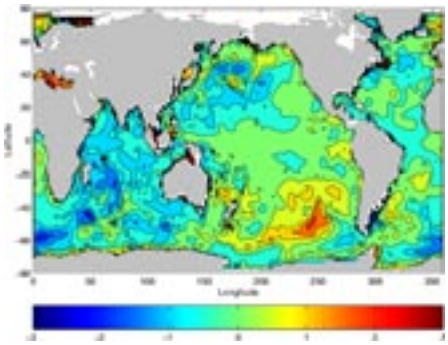

Figure 2. Constrained annual cycle amplitudes of bottom pressure minus unconstrained values (in equivalent centimeters of water). Contour line interval is 0.5 cm.

The optimization introduces substantial changes in p_b, compared with typical root-mean-square seasonal variability of 1 to 4 cm. For example, larger amplitudes are found in the Southern Ocean (Pacific sector), which is an important region for L_2 and also L_1 variability. Changes in the annual cycle of vertically-integrated currents, comparable to typical amplitudes of annual variability on the order of a few mm/s, are also apparent in many regions (not shown).

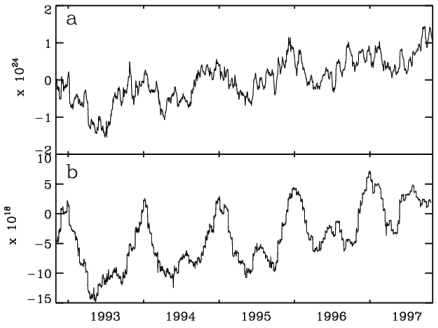

Figure 3. Constrained minus unconstrained values of **(a)** L_3 in kg m^2s^{-1} and **(b)** zonal wind stress torque over the ocean T_z in kg m^2s^{-2}.

Changes in OAM are ultimately related to the optimization of the control variables, particularly the wind fields and associated stress torques; e.g., some of the changes in L_3 can be traced to the zonal stress torque T_z (defined as the area integral of r cos ϕ τ^z where ϕ is latitude and τ^z is zonal stress).

The optimization leads to corrections in the seasonal cycle of T_z on the order of several Hadleys (1 Hadley=10^{18} kg m^2s^{-2}) and comparable to typical seasonal variability. The suggested large errors in T_z should impact on the axial atmospheric angular momentum (AAM) budget. In fact, comparisons of AAM tendency and torques show substantial imbalances at seasonal time scales, with amplitudes and signs not inconsistent with the results in Figure 3.

Planetary angular momentum budget

• **Excitation functions χ:**

$$(\chi_1, \chi_2) = [\Omega (C - A)]^{-1} [(L_1^P, L_2^P) + 1.43 (L_1^V, L_2^V)]$$

$$\chi_3 = (\Omega C)^{-1} (0.7 L_3^P + L_3^V)$$

C and A are the axial and equatorial moments of inertia of the mantle, respectively, and numerical factors represent elastic Earth effects, as formulated using Love numbers.

• Atmospheric excitation functions calculated based on NCEP/NCAR reanalysis products, with inverted barometer assumption used for mass terms and winds up to 10 hPa pressure level included for motion term

• Geodetic (observed) excitation functions based on pole positions from the International Earth Rotation Service and length-of-day (LOD) values from SPACE series from R. Gross (JPL)

Polar motion

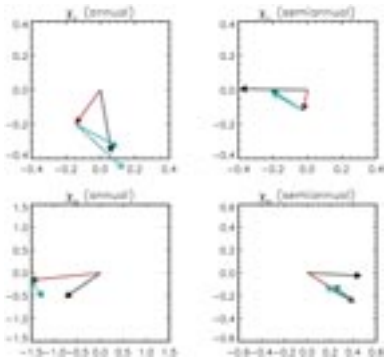

Figure 4. Phasor diagram for annual and semiannual wobble excitation in χ_1 (top) and χ_2 (bottom). Vectors represent dimensionless amplitude ($x10^{-7}$) and phase of χ^G (black), χ^A (red), and χ^O (blue). An arrow pointing due east (south) denotes a maximum on January 1 (April 1). χ^G and χ^A vectors share the origin, and χ^O is added to χ^A. Solid blue arrows denote constrained χ^O values.

There are large differences in constrained and unconstrained OAM values, particularly for the annual period: the assimilation leads to a large increase in the amplitude of χ_2 and a noticeable phase shift in χ_1, providing for substantially improved budget on the annual period. And, although weaker, the impact of the data assimilation likewise leads to reduced residuals on semiannual terms as well.

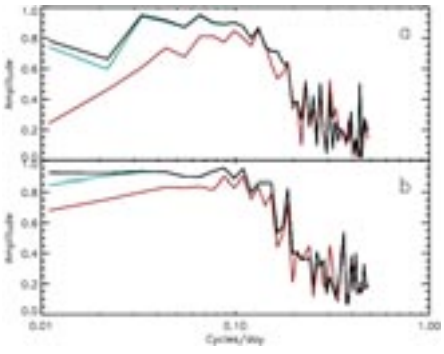

Figure 5. (a) Sub-seasonal coherence amplitudes between χ_1^G and χ_1^A (red), unconstrained χ_1^{O+A} (blue), and constrained χ_1^{O+A} (black). First point plotted represents the 6 to 2 month band. Coherence amplitudes larger than 0.38 are significantly different from zero at the 95% confidence level. **(b)** As in (a) but for χ_2 quantities.

Constrained OAM values provide slightly higher coherence amplitudes at periods >20 days. At shorter periods, the effects of optimization are negligible, as expected from the discussion of Figure 1.

For the periods ranging from annual to 20 days, time series of χ^{O+A} based on constrained OAM estimates can explain 71% and 75% of the variance in χ_1^G and χ_2^G, respectively, compared to only 66% and 65% for unconstrained estimates.

Length of day

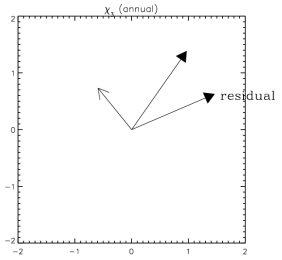

Figure 6. Phasor diagram for annual excitation in χ_3. Vectors represent dimensionless amplitudes ($x10^{-9}$) and phases of χ^{G-A} (residual curve) and χ^O. Solid arrow denotes constrained χ^O value. Phase is plotted as in Figure 4.

For the LOD budget, the optimization leads to a substantial change in the annual cycle (Figure 3), with constrained estimates having twice the amplitude and a phase which is shifted by more than 2 months relative to the unconstrained run. These differences lead to better agreement with the annual cycle of the residual χ^{G-A}, but we note that uncertainties in the latter residual are also substantial.

Summary

Analysis of OAM quantities calculated from output of a global model constrained by data (altimetry, monthly hydrography, and sea surface temperature) reveals a clear impact of the optimization procedure on the large scale (vertically averaged) circulation and mass fields. All three OAM components are substantially changed, particularly at seasonal timescales, providing for better agreement with observed signals in LOD and PM. The comparison with Earth rotation data attests to the beneficial impact of the estimation scheme on OAM values and constitutes a novel consistency check on the estimated oceanic large scale fields. The optimization also yields substantial adjustments to the seasonal wind stress fields, which can be checked in the context of the AAM budget.